

Resilient Continuum Deformation Coordination \star

Hossein Rastgoftar^a Ella Atkins^b

^a*Department of Aerospace Engineering, University of Michigan, Ann Arbor, MI, 48109 USA*

^b*Department of Aerospace Engineering, University of Michigan, Ann Arbor, MI, 48109 USA*

Abstract

This paper applies the principles of continuum mechanics to safely and resiliently coordinate a multi-agent team. A hybrid automation with two operation modes, Homogeneous Deformation Mode (HDM) and Containment Exclusion Mode (CEM), are developed to robustly manage group coordination in the presence of unpredicted agent failures. HDM becomes active when all agents are healthy, where the group coordination is defined by homogeneous transformation coordination functions. By classifying agents as leaders and followers, a desired n -D homogeneous transformation is uniquely related to the desired trajectories of $n+1$ leaders and acquired by the remaining followers in real-time through local communication. The paper offers a novel approach for leader selection as well as naturally establishing and reestablishing inter-agent communication whenever the agent team enters the HDM. CEM is activated when at least one agent fails to admit group coordination. This paper applies unique features of decentralized homogeneous transformation coordination to quickly detect each arising anomalous situation and excludes failed agent(s) from group coordination of healthy agents. In CEM, agent coordination is treated as an ideal fluid flow where the desired agents' paths are defined along stream lines inspired by fluid flow field theory to circumvent exclusion spaces surrounding failed agent(s).

Key words: Resilient Multi-agent Coordination, Physics-based Methods, Local Communication, Continuum Deformation, and Decentralized Control.

1 Introduction

Control of multi-agent systems has been widely investigated over the past two decades. Formation and cooperative control can reduce cost and improve the robustness and capability of reconfiguration in a cooperative mission. Therefore, researchers have been motivated to explore diverse applications for the multi-agent coordination such as formation control [32], traffic congestion control [30], distributed sensing, [12], cooperative surveillance [31], and cooperative payload transport [18].

1.1 Related Work

Centralized and decentralized cooperative control approaches have been previously proposed for multi-agent coordination. The virtual structure [25] [24] model treats agents as particles of a rigid body. Assuming the virtual body has an arbitrary translation and rigid body rotation in a 3-D motion space, the desired trajectory of ev-

ery agent is determined in a centralized fashion. Consensus [5] [14] [7] [3] [19] [1] [36] [15] [28] [34] and containment control are the most common decentralized coordination approaches. Multi-agent coordination using first-order consensus [16] and second-order consensus [5] [14] has been extensively investigated by researchers in the past. Leader-based and leaderless consensus have been studied in Refs. [7] and [3]. Stability of the retarded consensus method was studies in Refs. [19] [1]. Finite-time multi-agent consensus of continuous time systems is studied in Refs. [36] [15]. Refs. [28] [34] evaluate consensus under a switching communication topology in the presence of disturbances.

More recently, researchers have investigated the resilient consensus problem and provided guarantee conditions for reaching consensus in the presence of malicious agents [4, 9, 10, 26]. Weighted Mean Subsequence Reduced (W-MSR) is commonly used to detect an adversary and remove malicious agent(s) from the communication network of normal agents [4, 10]. r -robustness and (r, s) -robustness conditions are used to prove network resilience under consensus. Particularly, $(f + 1, f + 1)$ -robustness is considered as the necessary and sufficient condition for resilience of the consensus protocol in the

\star Authors are with the Department of Aerospace Engineering, University of Michigan, Ann Arbor, MI, 48109 USA e-mail: hosseinp@umich.edu.

presence of f malicious agents [4].

Containment control is a decentralized leader-follower approach in which multi-agent coordination is guided by a finite number of leaders and acquired by followers through local communication. Necessary and sufficient conditions for the stability of continuum deformation coordination have been provided in Refs. [17]. Ref. [6] studies the convergence of containment control and demonstrates that followers ultimately converge to the convex hull defined by leaders. Containment control under fixed and switching communication protocols are studied in Refs. [2] and [11], respectively. Refs. [29, 35] study finite-time containment stability and convergence. Containment control stability in the presence of communication delay is studied in Refs. [27, 33].

Continuum deformation for large-scale coordination of multi-agent systems is developed in [20]. Similar to containment control, continuum deformation is a leader-follower approach in which a group coordination is guided by a finite number of leaders and acquired by followers through local communication [22]. Because continuum deformation defines a non-singular mapping between reference and current agent configurations at any time t , follower communication weights are consistent with leader agents' reference positions in the continuum deformation coordination. The continuum deformation method advances containment control by formal characterization of safety in a large-scale coordination. Assuming continuum deformation is given by a homogeneous transformation, inter-agent collision and agent follower containment are guaranteed in a continuum deformation coordination by assigning a lower limit on the eigenvalues of the Jacobian matrix of the homogeneous transformation. Therefore, a large number of agents participating in a continuum deformation coordination can safely and aggressively deform to pass through narrow passages in a cluttered environment.

1.2 Contributions and Outline

This paper proposes a physics-inspired approach to the resilient multi-agent coordination problem. In particular, multi-agent coordination is modeled by a hybrid automation with two physics-based coordination modes: (i) Homogeneous Deformation Mode (HDM) and (ii) Containment Exclusion Mode (CEM).

HDM is active when all agents are healthy and can admit the desired coordination defined by a homogeneous deformation. In the HDM, agents are treated as particles of an n -D deformable body and the desired coordination, defined based on the trajectories of $n + 1$ leaders forming an n -D simplex at any time t , is acquired by the followers through local communication.¹

¹ This paper considers agents as particles of 2-D and 3-D

CEM is activated once an adversarial situation is detected due to unpredicted vehicle or agent failure. The paper offers a novel approach for rapid detection of each anomalous or failed agent and excludes it from group coordination with the healthy vehicles. In CEM the desired coordination is treated as an irrotational fluid flow and adversarial agents are excluded from the safe planning space by combining ideal fluid flow patterns in a computationally-efficient manner.

Compared to the existing literature and the authors' previous work, this paper offers the following contributions:

- (1) The paper offers a novel distributed approach for detection of anomalous situations in which unexpected vehicle failure(s) disrupt collective vehicle motion.
- (2) This paper advances the existing continuum deformation coordination theory by relaxing the follower containment constraint and offering a tetrahedralization approach to assign followers' communication weights in an unsupervised fashion.
- (3) The paper proposes a model-free guarantee condition for convergence and inter-agent collision avoidance in a large-scale homogeneous transformation.
- (4) Compared to existing resilient coordination work [9] [26] [4] [10], this paper offers a computationally-efficient safety recovery method. At CEM, every agent assigns its own desired trajectory without communication with other agents only by knowing the geometry of the unsafe domains enclosing the anomalous agents, as well as its own reference position when the CEM is activated.
- (5) This paper proposes a tetrahedralization method to (i) naturally establish/reestablish inter-agent communication links and weights, (ii) classify agents as boundary and follower agents, (iii) determine leaders in an unsupervised fashion.
- (6) The authors believe this is the first paper describing safe exclusion of a failed agent in a cooperative team with inspiration from fluid flow models.

This paper is organized as follows. Preliminaries in Section 2 are followed by a resilient continuum deformation formulation in Section 3. Physics-based models for the HDM and CEM are described in Section 4. Operation of the resilient continuum deformation coordination is modeled by a hybrid automation in Section 5. Simulation results presented in Section 6 are followed by concluding remarks in Section 7.

deformable bodies where 2-D and 3-D homogeneous deformation defines the desired coordination at the HDM. Therefore, n is either 2 or 3.

2 Preliminaries

2.1 Position Notations

The following position notations are used throughout this paper: Reference position of vehicle i is denoted by $\mathbf{r}_{i,0} = [x_{i,0} \ y_{i,0} \ z_{i,0}]^T$. In this paper, a reference configuration is defined based on agents' current positions once they enter the HDM. Actual position of vehicle i is denoted $\mathbf{r}_i(t) = [x_i(t) \ y_i(t) \ z_i(t)]^T$ at time t . Local desired position of vehicle i is denoted by $\mathbf{r}_{i,d}(t) = [x_{i,d}(t) \ y_{i,d}(t) \ z_{i,d}(t)]^T$ at time t . $\mathbf{r}_{i,d}$ is updated through local communication and defined based on actual positions of the in-neighbor vehicles of agent i . Global desired position of vehicle i is denoted by $\mathbf{r}_{i,c}(t) = [x_{i,c}(t) \ y_{i,c}(t) \ z_{i,c}(t)]^T$ at time t . The transient error is defined as the difference between actual position $\mathbf{r}_i(t)$ and global desired position $\mathbf{r}_{i,c}(t)$ for vehicle i at any time t .

2.2 Motion Space Tetrahedralization and Λ Operator

Assume $\mathbf{c} \in \mathbb{R}^{3 \times 1}$; $\mathbf{p}_1, \mathbf{p}_2, \dots, \mathbf{p}_{n+1} \in \mathbb{R}^{3 \times 1}$ are $n+1$ arbitrary position vectors in a 3-D motion space. Then, rank operator χ_n is defined as follows:

$$n = 2, 3, \quad \chi_n(\mathbf{p}_1, \dots, \mathbf{p}_n) = \text{rank} \left(\begin{bmatrix} \mathbf{p}_2 - \mathbf{p}_1 & \dots & \mathbf{p}_{n+1} - \mathbf{p}_1 \end{bmatrix} \right) \quad (1)$$

If $\mathbf{p}_1, \dots, \mathbf{p}_{n+1}$ are positioned at the vertices an n -D simplex, then $\chi_n(\mathbf{p}_1, \dots, \mathbf{p}_n) = n$. $\mathbf{p}_1, \mathbf{p}_2, \mathbf{p}_3$, and \mathbf{p}_4 form a tetrahedron for $n = 3$, if $\chi_3(\mathbf{p}_1, \mathbf{p}_2, \mathbf{p}_3, \mathbf{p}_4) = 3$. $\mathbf{p}_1, \mathbf{p}_2$, and \mathbf{p}_3 form a triangle for $n = 2$, if $\chi_2(\mathbf{p}_1, \mathbf{p}_2, \mathbf{p}_3) = 2$.

Operator Λ ($n = 2, 3$): Assume $\mathbf{p}_1, \mathbf{p}_2, \mathbf{p}_3$, and \mathbf{p}_4^n are known points in a 3-D motion space, where

$$\chi_3(\mathbf{p}_1, \mathbf{p}_2, \mathbf{p}_3, \mathbf{p}_4^n) = 3. \quad (2)$$

Then, operator Λ can be defined as follows:

$$n = 2, 3, \quad \Lambda(\mathbf{p}_1, \mathbf{p}_2, \mathbf{p}_3, \mathbf{p}_4^n, \mathbf{c}^n) = \begin{bmatrix} \mathbf{p}_1 & \mathbf{p}_2 & \mathbf{p}_3 & \mathbf{p}_4^n \\ 1 & 1 & 1 & 1 \end{bmatrix}^{-1} \begin{bmatrix} \mathbf{c}^n \\ 1 \end{bmatrix}, \quad (3)$$

where \mathbf{c}^n is the position of a point in a 3-D motion space. If $\chi_3(\mathbf{p}_1, \mathbf{p}_2, \mathbf{p}_3, \mathbf{p}_4^n) = 3$, $\Lambda(\mathbf{p}_1, \dots, \mathbf{p}_n, \mathbf{c}^n)$ exists and has the following properties [23]:

- (1) The sum of the entries of Λ is 1 for any configuration of vectors $\mathbf{p}_1, \dots, \mathbf{p}_4^n$ and \mathbf{c}^n for $n = 2, 3$.
- (2) If $\Lambda > \mathbf{0}$, \mathbf{c}^n is inside the tetrahedron formed by $\mathbf{p}_1, \dots, \mathbf{p}_4^n$. Otherwise, it is outside the tetrahedron.

Motion Space Tetrahedralization: A 3-D motion space can be divided into two subspaces that are inside

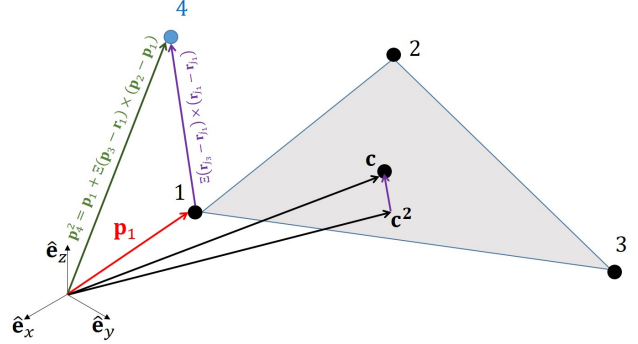


Figure 1. Graphical representation of the virtual agent \mathbf{p}_4^2 .

and outside of the tetrahedron defined by vectors $\mathbf{p}_1, \mathbf{p}_2, \mathbf{p}_3$, and \mathbf{p}_4^n , if $\chi_3(\mathbf{p}_1, \mathbf{p}_2, \mathbf{p}_3, \mathbf{p}_4^n) = 3$.

For $n = 3$, $\mathbf{p}_1, \mathbf{p}_2, \mathbf{p}_3, \mathbf{p}_4$, and \mathbf{c} represent real points (agents) in a 3-D motion space, if $\chi_3(\mathbf{p}_1, \mathbf{p}_2, \mathbf{p}_3, \mathbf{p}_4) = 3$. Therefore, $\mathbf{p}_4^3 = \mathbf{p}_4$ and $\mathbf{c}^3 = \mathbf{c}$.

For $n = 2$, $\mathbf{p}_1, \mathbf{p}_2$, and \mathbf{p}_3 are the real points forming a triangle in a 3-D motion space. Given $\mathbf{p}_1, \mathbf{p}_2$, and \mathbf{p}_3 , virtual point

$$\mathbf{p}_4^2 = \mathbf{p}_1 + \Xi(\mathbf{p}_3 - \mathbf{p}_1) \times (\mathbf{p}_2 - \mathbf{p}_1), \quad (4)$$

where $\Xi \neq 0$ is constant. Note that \mathbf{p}_4^2 , defined by Eq. (4), is perpendicular to the triangular plane made by agents $\mathbf{p}_1, \mathbf{p}_2$, and \mathbf{p}_3 (see Fig. 1). Consequently, virtual agent \mathbf{p}_4^2 and in-neighbor agent $\mathbf{p}_1, \mathbf{p}_2$, and \mathbf{p}_3 form a tetrahedron. The projection of \mathbf{c} on the triangular plane made by $\mathbf{p}_1, \mathbf{p}_2$, and \mathbf{p}_3 is denoted by $\tilde{\mathbf{c}}^2$ and expressed as follows:

$$\mathbf{c}^2 = \mathbf{c} - (\mathbf{c} \cdot \mathbf{n}_{1-4}(\mathbf{p}_1, \mathbf{p}_2, \mathbf{p}_3)) \mathbf{n}_{1-4}(\mathbf{p}_1, \mathbf{p}_2, \mathbf{p}_3), \quad (5)$$

where unit vector

$$\mathbf{n}_{1-4}(\mathbf{p}_1, \mathbf{p}_2, \mathbf{p}_3) = \frac{(\mathbf{p}_3 - \mathbf{p}_1) \times (\mathbf{p}_2 - \mathbf{p}_1)}{\|(\mathbf{p}_3 - \mathbf{p}_1) \times (\mathbf{p}_2 - \mathbf{p}_1)\|} \quad (6)$$

is normal to the triangular plane made by $\mathbf{p}_1, \mathbf{p}_2$, and \mathbf{p}_3 .

Proposition 1. Let Λ be expressed in component-wise form:

$$\Lambda = [\lambda_1 \ \lambda_2 \ \lambda_3 \ \lambda_4]^T.$$

If $n = 2$, $\lambda_4(\mathbf{p}_1, \mathbf{p}_2, \mathbf{p}_3, \mathbf{p}_4^2, \mathbf{c}^2) = 0$ for any arbitrary position \mathbf{c}^2 .

Proof. Given $\mathbf{p}_1, \mathbf{p}_2, \mathbf{p}_3$, and \mathbf{p}_4^n , $\lambda_4(\mathbf{p}_1, \mathbf{p}_2, \mathbf{p}_3, \mathbf{p}_4^n, \mathbf{c}^n)$ is obtained as follows:

$$\lambda_4(\mathbf{p}_1, \mathbf{p}_2, \mathbf{p}_3, \mathbf{p}_4^n, \mathbf{c}^n) = \frac{\|\mathbf{c}^n - \mathbf{c}^2\|}{\|\mathbf{p}_4^n - \mathbf{p}_1\|}. \quad (7)$$

For $n = 2$, the denominator of Eq. (7) is 0, thus $\lambda_4(\mathbf{p}_1, \mathbf{p}_2, \mathbf{p}_3, \mathbf{p}_4^n, \mathbf{c}^n) = 0$ for any arbitrary position of point \mathbf{c} in the motion space. \square

Operator Λ will be used to (i) determine boundary and interior agents, (ii) specify followers' in-neighbor agents, (iii) assign followers' communication weights in a 2-D and 3-D homogeneous deformation coordination, and (iv) detect anomalies in a group coordination.

2.3 Homogeneous Deformation

A homogeneous deformation is an affine transformation² given by

$$\mathbf{r}_{i,c}(t) = \mathbf{Q}(t)\mathbf{r}_{i,0} + \mathbf{d}(t), \quad (8)$$

where $\mathbf{Q}(t)$ is the Jacobian matrix, $\mathbf{d}(t)$ is the rigid-body displacement vector, $\mathbf{r}_{i,0}$ is the reference position of agent $i \in \mathcal{V}_H(t)$, and $\mathcal{V}_H(t)$ defines index numbers of healthy agents at time t .

α parameters: Let $\mathcal{V}_H(t)$ be expressed as

$$\mathcal{V}_H = \mathcal{V}_L \bigcup \mathcal{V}_F. \quad (9)$$

where $\mathcal{V}_L = \{i_1, \dots, i_{n+1}\}$ and $\mathcal{V}_F(t) = \{i_{n+2}, \dots, i_{N_F}\}$ are disjoint sets defining leaders and followers at time t . Let $\mathbf{r}_{i_1,0}, \dots, \mathbf{r}_{i_{n+1},0}$ denote the reference positions of the leaders and $\mathbf{r}_{i_j,0}$ denotes the reference position of follower $i_j \in \mathcal{V}$, where reference positions are all assigned at the time agents first enter HDM. Then, we can define α parameters α_{i_j, i_1} through α_{i_j, i_4} as follows:

$$\begin{bmatrix} \alpha_{i_j, i_1} & \dots & \alpha_{i_j, i_4} \end{bmatrix}^T = \Lambda \left(\mathbf{r}_{i_1,0}, \mathbf{r}_{i_2,0}, \mathbf{r}_{i_3,0}, \mathbf{r}_{i_4,0}^n, \mathbf{r}_{i_j,0}^n \right), \quad (10)$$

where

$$\mathbf{r}_{i_4,0}^n = \begin{cases} \mathbf{r}_{i_4,0} & n = 3 \\ \mathbf{r}_{i_1,0} + \Xi(\mathbf{r}_{i_3,0} - \mathbf{r}_{i_1,0}) \times (\mathbf{r}_{i_2,0} - \mathbf{p}_{i_1,0}) & n = 2 \end{cases}, \quad (11a)$$

$$\mathbf{r}_{i_j,0}^n = \begin{cases} \mathbf{r}_{i_j,0} & n = 3 \\ \mathbf{r}_{i_j,0} - (\mathbf{r}_{i_j,0} \cdot \mathbf{n}_{1-4}) \mathbf{n}_{1-4} & n = 2 \end{cases}, \quad (11b)$$

and $\mathbf{n}_{1-4} = \mathbf{n}_{1-4}(\mathbf{r}_{i_1,0}, \mathbf{r}_{i_2,0}, \mathbf{r}_{i_3,0})$ was previously defined in (6). Note that $\alpha_{i_1, i_4} = 0$, if $n = 2$ (See Proposition 1).

Global Desired Position: Because homogeneous deformation is a linear transformation, global desired position of vehicle i_j can be either given by Eq. (8) or expressed

² The affine transformation (8) is called *Homogeneous Deformation* in continuum mechanics [8].

as a convex combination of the leaders' positions at any time t .

$$j \in \mathcal{V}_F, \quad \mathbf{r}_{j,c} = \sum_{k=1}^{n+1} \alpha_{j,i_k} \mathbf{r}_{i_k,c}(t). \quad (12)$$

3 Problem Formulation and Statement

Consider a 3-D motion space containing M agents where every agent is uniquely identified by a number $i \in \mathcal{M} = \{1, \dots, M\}$. It is assumed that $N(t)$ (out of M) agents are enclosed by a rigid-size *containment domain*

$$\Omega_{\text{con}} = \Omega_{\text{con}}(\mathbf{r}, \mathbf{r}_{\text{con}}(t)) \subset \mathbb{R}^3, \quad (13)$$

at time t . Let $\mathbf{r}_{\text{con}}(t) \in \mathbb{R}^{3 \times 1}$ be the nominal position of the containment domain given by

$$\mathbf{r}_{\text{con}}(t) = \sum_{i=1}^{N(t)} \beta_i \mathbf{r}_{i,c}(t). \quad (14)$$

Note that $0 \leq \beta_i < 1$ is a scaling factor, $\sum_{i=1}^{N(t)} \beta_i = 1$, and the size of $\Omega_{\text{con}} = \Omega_{\text{con}}(\mathbf{r}, \mathbf{r}_{\text{con}}(t)) \subset \mathbb{R}^3$ does not change over time. Identification numbers of the agents enclosed by $\Omega_{\text{con}}(t)$ are defined by set

$$\mathcal{V}(t) = \{i \in \mathcal{M} | \mathbf{r}_{i,c}(t) \in \Omega_{\text{con}}(\mathbf{r}, \mathbf{r}_{\text{con}}(t))\} \quad (15)$$

Agents enclosed by the containment region $\Omega_{\text{con}}(\mathbf{r}, \mathbf{r}_{\text{con}}(t))$ can be classified as *healthy* or *anomalous* agents, where *healthy* agents admit the group desired coordination while *anomalous* agents do not. *Healthy* and *anomalous* vehicles are defined by disjoint sets \mathcal{V}_H and \mathcal{V}_A , respectively, where \mathcal{V} can be expressed as

$$\mathcal{V} = \mathcal{V}_H \bigcup \mathcal{V}_A, \quad (16)$$

where $\mathcal{V}_H = \{i_1, \dots, i_{N_F}\}$ and $\mathcal{V}_A = \{i_{N_F+1}, \dots, i_N\}$.

This paper treats agents as particles of a deformable body where the desired trajectory of vehicle $j \in \mathcal{V}$ is given by

$$\dot{\mathbf{r}}_{j,c}(x_{j,c}, y_{j,c}, z_{j,c}, t) = \mathbf{H}_{j,\gamma}(x_{j,c}, y_{j,c}, z_{j,c}) \dot{\mathbf{q}}_\gamma(t), \quad (17)$$

where γ is a discrete variable defined by finite set $\Gamma = \{\text{CEM}, \text{HDM}\}$. Set Γ specifies the collective motion operation mode. $\mathbf{r}_{j,c}(t) = [x_{j,c}(t) \ y_{j,c}(t) \ z_{j,c}(t)]^T$ is the global desired trajectory of vehicle j , $\mathbf{q} = [q_{1,\gamma} \ \dots \ q_{m,\gamma}(t)]^T$, $q_{1,\gamma}(t)$ through $q_{N,\gamma}(t)$ are the **generalized coordinates** specifying the temporal behavior of the group coordination. Furthermore,

$$j \in \mathcal{V}, \quad \gamma \in \Gamma, \quad \mathbf{H}_{j,\gamma} = [\mathbf{h}_{j,1,\gamma} \ \dots \ \mathbf{h}_{j,m,\gamma}] \in \mathbb{R}^{3 \times m}$$

is the spatially-varying **shape matrix**. $\mathbf{h}_{j,1,\gamma}(x_{j,c}, y_{j,c}, z_{j,c}) \in \mathbb{R}^{3 \times 1}$ through $\mathbf{h}_{j,m,\gamma}(x_{j,c}, y_{j,c}, z_{j,c}) \in \mathbb{R}^{3 \times 1}$ are the **shape functions**.

HDM ($\gamma = \text{HDM}$) is active when $\mathcal{V}_A = \emptyset$. Therefore, $N_F(t) = N(t)$ agents defined by set \mathcal{V}_H are all healthy. The HDM shape matrix $\mathbf{H}_{j,\text{HDM}}$ is time-invariant (constant), where $j \in \mathcal{V}_H$. The HDM generalized coordinate vector $\mathbf{q}_{\text{HDM}} \in \mathbb{R}^{3(n+1) \times 1}$ specifies desired velocity components of all leaders guiding the group continuum deformation coordination. This paper develops a decentralized leader-follower approach using the tetrahedralization presented in Section 2.2. By classifying agents as leaders and followers, $\mathcal{V}_H = \mathcal{V}_L \cup \mathcal{V}_F$ (See Eq. (9)). Leaders, defined by $\mathcal{V}_L = \{i_1, \dots, i_{n+1}\}$, move independently. Followers, defined by $\mathcal{V}_F = \{i_{n+2}, \dots, i_N\}$, acquire the desired coordination through local communication with leaders and other followers. The paper offers a tetrahedralization method to determine leaders and followers and define inter-agent communication among vehicles in an unsupervised fashion for an arbitrary reference configuration of agents.

CEM ($\gamma = \text{CEM}$) is activated once at least one anomalous agent is detected in which case $\mathcal{V}_A \neq \emptyset$. The CEM shape matrix $\mathbf{H}_{j,\text{CEM}}$ ($j \in \mathcal{V}_H$) is spatially varying. In particular, the desired vehicle coordination of healthy vehicle $j \in \mathcal{V}_H$ is defined by an ideal fluid flow. For CEM, it is desired that (i) vehicle $j \in \mathcal{V}_H$ moves along the surface $z_{j,c} = z_j(x_{j,c}, y_{j,c}, t)$ and (ii) x and y components of the agent coordination are defined by an irrotational flow. Mathematically speaking, we define coordinate transformation

$$\begin{cases} \phi_{j,c} = \phi(x_{j,c}, y_{j,c}, t) \\ \psi_{j,c} = \psi(x_{j,c}, y_{j,c}, t) \\ z_{j,c} = z_j(x_{j,c}, y_{j,c}, t) \end{cases}, \quad (18)$$

where $j \in \mathcal{V}_H$, $\phi(x_{j,c}, y_{j,c}, t)$ and $\psi(x_{j,c}, y_{j,c}, t)$ satisfy the Laplace equation:

$$\frac{\partial^2 \phi(x_{j,c}, y_{j,c}, t)}{\partial x_{j,c}^2} + \frac{\partial^2 \phi(x_{j,c}, y_{j,c}, t)}{\partial y_{j,c}^2} = 0 \quad (19a)$$

$$\frac{\partial^2 \psi(x_{j,c}, y_{j,c}, t)}{\partial x_{j,c}^2} + \frac{\partial^2 \psi(x_{j,c}, y_{j,c}, t)}{\partial y_{j,c}^2} = 0. \quad (19b)$$

For smooth "flow" every agent $j \in \mathcal{V}_H$ slides along the j -th streamline defined by $j \in \mathcal{V}_H$, $\psi(x_{j,c}, y_{j,c}, t) = \psi_{j,0} = \text{constant}$ at any time t . This condition requires that the desired trajectory of vehicle $j \in \mathcal{V}_H$ satisfy the following equation at any time t :

$$\frac{\partial \psi(x_{j,c}, y_{j,c}, t)}{\partial x_{j,c}} \frac{dx_{j,c}}{dt} + \frac{\partial \psi(x_{j,c}, y_{j,c}, t)}{\partial y_{j,c}} \frac{dy_{j,c}}{dt} = 0. \quad (20)$$

Notice that stream and potential functions satisfy the Cauchy-Riemann condition. Therefore, the level curves $\phi(x, y, t) = \text{constant}$ and $\psi(x, y, t) = \text{constant}$ are perpendicular at the intersection point. This paper defines $\phi(x, y, t)$ and $\psi(x, y, t)$ by combining ideal fluid flow patterns so that an obstacle-free motion space is excluded from adversaries. This combination can split the $x - y$ plane into a safe region defined by set \mathcal{S} and unsafe region defined by set \mathcal{U} . A one-to-one mapping exists between (x_j, y_j) and $(\phi(x_j, y_j), \psi(x_j, y_j))$ at every point in the safe set \mathcal{S} . Thus, the Jacobian matrix

$$(x, y) \in \mathcal{S}, j \in \mathcal{V}_H \quad \mathbf{J}(x_j, y_j) = \begin{bmatrix} \frac{\partial \phi}{\partial x_j} & \frac{\partial \phi}{\partial y_j} \\ \frac{\partial \psi}{\partial x_j} & \frac{\partial \psi}{\partial y_j} \end{bmatrix} \quad (21)$$

is nonsingular. Potential and stream fields are generated by combining "Uniform" and "Doublet" flow patterns. As a result, a single failed vehicle can be separated by a cylinder from the safe region \mathcal{S} in the motion space.

This paper also offers a novel distributed anomaly detection approach by using the properties of leader-follower homogeneous transformation coordination. Particularly, the Λ operator is used to characterize agent deviation of agents from the desired coordination to quickly identify failed agent(s) that are not admitting the desired continuum deformation.

4 Physics-based Modeling of HDM and CEM

HDM and CEM are mathematically modeled in this section. A decentralized leader follower method for HDM is developed in Section 4.1 to acquire a desired continuum deformation in an unsupervised fashion. CEM coordination is modeled in Section 4.2.

4.1 Homogeneous Deformation Mode (HDM)

In HDM, vehicles are healthy and cooperative. Therefore, $|\mathcal{V}_A| = 0$ ($N_F = N$ and $\mathcal{V}_H = \mathcal{V}$). Set \mathcal{V}_H can be expressed as $\mathcal{V}_H = \mathcal{V}_L \cup \mathcal{V}_F$, where $\mathcal{V}_L = \{i_1, \dots, i_{n+1}\}$ and $\mathcal{V}_F = \{i_{n+2}, \dots, i_N\}$ define leaders and followers, respectively.

4.1.1 Desired Homogeneous Deformation Definition

A desired homogeneous transformation can be defined by $m = 3(n+1)$ generalized coordinates $q_{1,\text{HDM}}, \dots, q_{3(n+1),\text{HDM}}$ using relation (17), where

$$\mathbf{q}_{\text{HDM}}(t) = \begin{bmatrix} q_{1,\text{HDM}}(t) \\ \vdots \\ q_{3(n+1),\text{HDM}}(t) \end{bmatrix} = \text{vec} \left(\begin{bmatrix} x_{i_1,c} & \cdots & x_{i_{n+1},c} \\ y_{i_1,c} & \cdots & y_{i_{n+1},c} \\ z_{i_1,c} & \cdots & z_{i_{n+1},c} \end{bmatrix}^T \right), \quad (22a)$$

$$\mathbf{H}_{i_j, \text{HDM}} = \begin{bmatrix} \mathbf{h}_{j,1} & \cdots & \mathbf{h}_{j,3(n+1)} \end{bmatrix} = \mathbf{I}_3 \otimes \begin{bmatrix} \alpha_{j,i_1} & \cdots & \alpha_{j,i_{n+1}} \end{bmatrix}, \quad (22b)$$

and $j \in \mathcal{V}$. Note that $\text{vec}(\cdot)$ is the matrix vectorization operator. In Section 2.3, it was described how α parameters α_{j,i_1} through $\alpha_{j,i_{n+1}}$ are assigned based on the agents' reference positions.

4.1.2 Unsupervised Acquisition of a Homogeneous Deformation Using Tetrahedralization

A desired homogeneous deformation, defined by $n + 1$ leaders in an n -D homogeneous deformation, is acquired by followers through local communication. Communication among healthy agents is defined by **coordination graph** $\mathcal{G}_c(\mathcal{V}, \mathcal{E})$ with nodes \mathcal{V} ($\mathcal{V} = \mathcal{V}_H$) and edges $\mathcal{E} \subset \mathcal{V} \times \mathcal{V}$. In-neighbor agents of agent $i \in \mathcal{V}$ are defined by

$$i \in \mathcal{V}, \quad \mathcal{N}_i = \{j | (j, i) \in \mathcal{E}\}.$$

Assuming the reference formation of agents is known, $n + 1$ boundary agents are selected as leaders. Furthermore, every follower $i \in \mathcal{V}_F$ communicates with $n + 1$ in-neighbor agents where the in-neighbor agents are placed at the vertices of an n -simplex containing follower i .

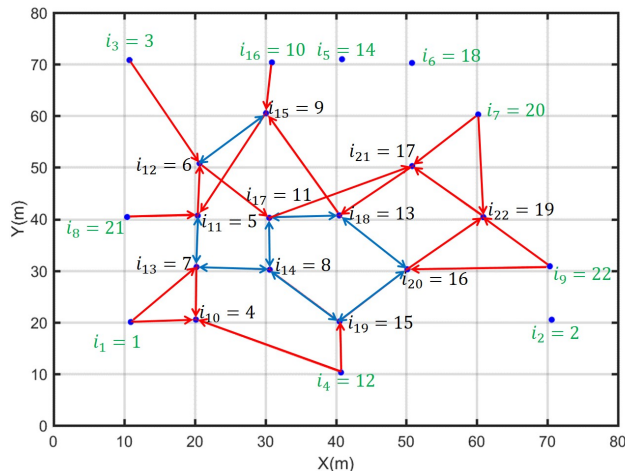


Figure 2. Example reference formation used for collective motion simulation. A red arrow shows a unidirectional link to a follower from its in-neighbor agent. Blue arrows show bidirectional communication.

4.1.3 Classification of Agents as Leaders and Followers

The node set \mathcal{V} can be expressed as $\mathcal{V} = \mathcal{V}_B \cup \mathcal{V}_I$ where $\mathcal{V}_B = \{i_1, \dots, i_{m_B}\}$ and $\mathcal{V}_I = \{i_{m_B+1}, \dots, i_N\}$ define boundary and interior agents, respectively. Given agents' reference positions, the following true statements are used to assign agent $i \in \mathcal{V}$ either as a leader or a follower:

- (1) An n -D homogeneous deformation is defined by $n + 1$ leaders [20, 21]. Assuming leaders are selected from the boundary agents, $\mathcal{V}_L \subset \mathcal{V}_B$.
- (2) Non-leader boundary agents are the followers specified by $(\mathcal{V}_B \setminus \mathcal{V}_L) \subset \mathcal{V}_F$.
- (3) All interior agents are followers, thus, $\mathcal{V}_I \subset \mathcal{V}_F$.
- (4) Agent i is an interior agent and classified as a follower, if there exists a set of three agents j_1, j_2 , and j_{n+1} such that $\Lambda(\mathbf{r}_{j_1,0}, \mathbf{r}_{j_2,0}, \mathbf{r}_{j_3,0}, \mathbf{r}_{j_4,0}, \mathbf{r}_{i,0}^n) > 0$, where $\mathbf{r}_{j_4,0}^n$ and $\mathbf{r}_{i,0}^n$ are assigned by Eq. (11) when subscripts i_1, i_2, i_3, i_4 , and i_j are substituted by j_1, j_2, j_3, j_4 , and i , respectively [23].
- (5) Assume $\Lambda(\mathbf{r}_{j_1,0}, \mathbf{r}_{j_2,0}, \mathbf{r}_{j_3,0}, \mathbf{r}_{j_4,0}, \mathbf{r}_{i,0}^n)$ has at least one negative entry for every $j_1, \dots, j_{n+1} \in \mathcal{V}$ forming an n -D simplex, where $j_1 \neq i, \dots$, and $j_{n+1} \neq i$. Then, $i \in \mathcal{V}$ is a boundary agent [23].
- (6) If $i \in \mathcal{V}$ is not a follower agent, it is a boundary agent.
- (7) Any $n + 1$ boundary agents j_1, \dots, j_{n+1} can be selected as leaders. The remaining boundary agents are also considered as the followers.

To better clarify the above statements, the reference formation shown in Fig. 2 is considered. The vehicle team consists of 22 agents ($\mathcal{V} = \{1, \dots, 22\}$). Set $\mathcal{V}_B = \{i_1, \dots, i_{10}\}$ define the boundary agents, where $i_1 = 1, i_2 = 2, i_3 = 3, i_4 = 10, i_5 = 12, i_6 = 14, i_7 = 18, i_8 = 20, i_9 = 21, i_{10} = 22$. While $\mathcal{V}_L = \{i_1, i_2, i_3\}$ specifies the leaders, $\mathcal{V}_B \subset \mathcal{V}_L$ defines the boundary followers. Boundary followers all communicate with leaders 1, 2, and 3. Note that links from leaders i_1, i_2 , and i_3 to boundary followers are not shown in Fig. 2. Additionally, $\mathcal{V}_I = \{i_{11}, \dots, i_{22}\}$ defines interior agents, where $i_{11} = 4, i_{12} = 5, i_{13} = 6, i_{14} = 7, i_{15} = 8, i_{16} = 9, i_{17} = 11, i_{18} = 13, i_{19} = 15, i_{20} = 16, i_{21} = 17$, and $i_{22} = 19$ are the interior vehicles. Note that $\mathcal{V}_I \subset \mathcal{V}_F$ are all followers.

4.1.4 Followers' In-Neighbors, Communication Weights, and HDM Desired Trajectories

The agent-tetrahedralization is used in this section to determine in-neighbor agents of interior followers in a homogeneous deformation coordination. For every **interior follower agent** $h \in \mathcal{V}_I \subset \mathcal{V}_F$, let

$$\mathcal{F}_h = \left\{ (j_1, \dots, j_{n+1}) \in \underbrace{\mathcal{V} \times \dots \times \mathcal{V}}_{n+1 \text{ times}} \mid \Lambda(\mathbf{r}_{j_1,0}, \dots, \mathbf{r}_{j_{n+1},0}, \mathbf{r}_{h,0}^n) > \varrho_n \mathbf{1}_4 \right\} \quad (23)$$

define admissible n -D simplexes enclosing interior follower h , where $\mathbf{1}_4 \in \mathbb{R}^{4 \times 1}$ is the one-entry vector and $\varrho > 0$ is constant.

Proposition 2. Positive parameter ϱ_n must be less than $\frac{1}{n+1}$ in an n -D homogeneous deformation ($n = 2, 3$).

Proof. For $n - D$ homogeneous transformation,

$$\begin{aligned} \mathbf{1}_4^T \mathbf{\Lambda} \left(\mathbf{r}_{j_1,0}, \dots, \mathbf{r}_{j_4,0}^n, \mathbf{r}_{h,0}^n \right) &= \sum_{l=1}^4 \lambda_l \left(\mathbf{r}_{j_1,0}, \dots, \mathbf{r}_{j_4,0}^n, \mathbf{r}_{h,0}^n \right) = \\ \sum_{l=1}^{n+1} \lambda_l \left(\mathbf{r}_{j_1,0}, \dots, \mathbf{r}_{j_4,0}^n, \mathbf{r}_{h,0}^n \right) &= 1 \end{aligned}$$

and

$$\varrho_n \leq \lambda_l \left(\mathbf{r}_{j_1,0}, \dots, \mathbf{r}_{j_4,0}^n, \mathbf{r}_{h,0}^n \right)$$

for $l = 1, \dots, n+1$, if $(j_1, j_2, j_3, j_4) \in \mathcal{F}_h$. Thus,

$$(n+1)\varrho_n < \sum_{l=1}^{n+1} \lambda_l \left(\mathbf{r}_{j_1,0}, \dots, \mathbf{r}_{j_4,0}^n, \mathbf{r}_{h,0}^n \right) = 1$$

which in turn implies that $\varrho_n < \frac{1}{n+1}$. \square

In-neighbors of an interior follower $h \in \mathcal{V}_I$ is defined by set $\mathcal{N}_h = \{j_1^*, \dots, j_{n+1}^*\}$, where

$$(j_1^*, \dots, j_{n+1}^*) = \underset{(j_1, \dots, j_{n+1}) \in \mathcal{F}_h}{\operatorname{argmin}} \sum_{k=1}^{n+1} \|\mathbf{r}_{j_k,0} - \mathbf{r}_{h,0}\|.$$

In other words, the $n+1$ closest agents belonging to set \mathcal{F}_h are considered as the in-neighbors of follower $h \in \mathcal{V}_F$.

Every boundary follower agent $j \in \mathcal{V}_B \setminus \mathcal{V}_L$ communicates with $n+1$ leaders defined by \mathcal{V}_L . Therefore, $\mathcal{N}_j = \mathcal{V}_L$ defines in-neighbor agent of vehicle $j \in \mathcal{V}_L \subset \mathcal{V}_B$.

Followers' Communication Weights: Each communication weight w_{i,j_k} ($k = 1, \dots, n+1$) is specified based on reference positions of follower vehicle $i \in \mathcal{V}_F$ and in-neighbor vehicle $j_k \in \mathcal{N}_i = \{j_1, \dots, j_{n+1}\}$ as follows:

$$\begin{bmatrix} w_{i,j_1} & \dots & w_{i,j_{n+1}} \end{bmatrix}^T = \mathbf{\Lambda} \left(\mathbf{r}_{j_1,0}, \mathbf{r}_{j_2,0}, \mathbf{r}_{j_3,0}, \mathbf{r}_{j_4,0}^n, \mathbf{r}_{i,0}^n \right), \quad (24)$$

where

$$\mathbf{r}_{j_4,0}^n = \begin{cases} \mathbf{r}_{j_4,0} & n = 3 \\ \mathbf{r}_{j_1,0} + \Xi(\mathbf{r}_{j_3,0} - \mathbf{r}_{j_1,0}) \times (\mathbf{r}_{j_2,0} - \mathbf{p}_{j_1,0}) & n = 2 \end{cases}, \quad (25a)$$

$$\mathbf{r}_{i,0}^n = \begin{cases} \mathbf{r}_{i,0} & n = 3 \\ \mathbf{r}_{i,0} - (\mathbf{r}_{i,0} \cdot \mathbf{n}_{1-4}) \mathbf{n}_{1-4} & n = 2 \end{cases}, \quad (25b)$$

and $\mathbf{n}_{1-4} = \mathbf{n}_{1-4}(\mathbf{r}_{j_1,0}, \mathbf{r}_{j_2,0}, \mathbf{r}_{j_3,0})$ is determined using Eq. (6) when $n = 2$. Given followers' communication weights, the weight matrix $\mathbf{W} = [W_{jh}] \in \mathbb{R}^{(N-n-1) \times N}$ is defined as follows:

$$W_{jh} = \begin{cases} w_{i_j, i_h} & i_h \in \mathcal{N}_j \wedge i_j \in \mathcal{V}_F \\ 0 & \text{otherwise} \end{cases} \quad (26)$$

Matrix \mathbf{W} can be partitioned as follows:

$$\mathbf{W} = \begin{bmatrix} \mathbf{B} | \mathbf{A} \end{bmatrix}, \quad (27)$$

where $\mathbf{B} \in \mathbb{R}^{(N-n-1) \times (n+1)}$ and $\mathbf{A} \in \mathbb{R}^{(N-n-1) \times (N-n-1)}$ are non-negative matrices.

HDM Desired Trajectory: Local desired trajectory of agent $i \in \mathcal{V}$ is defined as follows:

$$\mathbf{r}_{i,d}(t) = \begin{cases} \mathbf{r}_{i,c} & i \in \mathcal{V}_L \\ \sum_{h \in \mathcal{N}_i} w_{i,h} \mathbf{r}_h & i \in \mathcal{V}_F \end{cases}. \quad (28)$$

Note that global and local desired positions of leader agent $j \in \mathcal{V}_L$ are the same at any time t . The component $\mu \in \{x, y, z\}$ of the local desired positions of followers satisfy the following relation:

$$\mu \in \{x, y, z\}, \forall t, \quad \mathbf{P}_{\mu,d}^F(t) = \mathbf{A} \mathbf{P}_{\mu}^F(t) + \mathbf{B} \mathbf{P}_{\mu}^L(t), \quad (29)$$

where \mathbf{A} and \mathbf{B} were previously introduced in Eq. (27). $\mathbf{P}_{\mu}^L = [\mu_{i_1} \dots \mu_{i_{n+1}}]^T$, and $\mathbf{P}_{\mu}^F = [\mu_{i_{n+2}} \dots \mu_{i_N}]^T$ assign the component $\mu \in \{x, y, z\}$ of actual positions of leaders and followers, respectively. Furthermore, $\mathbf{P}_{\mu,d}^F = [\mu_{i_{n+2},d} \dots \mu_{i_N,d}]^T$ assigns component $\mu \in \{x, y, z\}$ of the local desired positions for all followers.

Key Property of Homogeneous Deformation: If followers' communication weights are consistent with agents' reference positions and obtained by Eq. (24), then, the following relation is true:

$$\mathbf{W}_L = -\mathbf{D}^{-1} \mathbf{B} = \begin{bmatrix} \alpha_{i_{n+2},i_1} & \dots & \alpha_{i_{n+2},i_{n+1}} \\ \vdots & \ddots & \vdots \\ \alpha_{i_N,i_1} & \dots & \alpha_{i_N,i_{n+1}} \end{bmatrix} \quad (30)$$

where

$$\mathbf{D} = -\mathbf{I} + \mathbf{A}$$

is Hurwitz (See the proof in Ref. [20]). Let $\mathbf{P}_{\mu,c}^L = [\mu_{i_1,c} \dots \mu_{i_{n+1},c}]^T$ and $\mathbf{P}_{\mu,c}^F = [\mu_{i_{n+2},c} \dots \mu_{i_N,c}]^T$ specify component $\mu \in \{x, y, z\}$ of the global desired positions of leaders and followers, respectively. Given the global desired position of followers defined by Eq. (12), $\mathbf{P}_{\mu,c}^F$ is defined based on $\mathbf{P}_{\mu,c}^L$ by

$$\mu \in \{x, y, z\}, \forall t, \quad \mathbf{P}_{\mu,c}^F(t) = \mathbf{W}_L \mathbf{P}_{\mu,c}^L(t). \quad (31)$$

Lemma 1. Every entry of matrix \mathbf{D}^{-1} is non-positive.

Proof. Diagonal entries of matrix \mathbf{D} are all -1 while the off-diagonal entries of \mathbf{D} are either 0 or positive. Using the Gauss-Jordan elimination method, the augmented

matrix $\mathbf{D}_a = [\mathbf{D}|\mathbf{I}] \in \mathbb{R}^{(N-n-1) \times 2(N-n-1)}$ can be converted to matrix $\tilde{\mathbf{D}}_a = [\mathbf{I}|\mathbf{D}^{-1}] \in \mathbb{R}^{(N-n-1) \times 2(N-n-1)}$ only by performing row algebraic operations. Entries of the lower triangle of matrix \mathbf{D} can be all converted to 0, if a top row is multiplied by a negative scalar and the outcome is added to the other rows. Elements of the upper triangular submatrix of \mathbf{L} can be similarly zeroed, if the bottom row is multiplied by a negative scalar and the outcome is added to the other rows. Therefore, \mathbf{D}^{-1} , obtained by performing these row operations on $\tilde{\mathbf{D}}_a$, is non-negative. \square

Lemma 2. Define the **local-desired error vector** $\mathbf{E}_{\mu,d}^F = [\mu_{i_{n+2},d} - \mu_{i_{n+2}} \cdots \mu_{i_N,d} - \mu_{i_N}]^T$, and the **global-desired error vectors** $\mathbf{E}_{\mu,c}^L = [\mu_{i_1,c} - \mu_{i_1} \cdots \mu_{i_{n+1},c} - \mu_{i_{n+1},d}]^T$ Considering Eq. (32b), we can write and $\mathbf{E}_{\mu,c}^F = [\mu_{i_{n+2},c} - \mu_{i_{n+2}} \cdots \mu_{i_N,c} - \mu_{i_N}]^T$ where $\mu \in \{x, y, z\}$. The following relations are true:

$$\mu \in \{x, y, z\}, \forall t, \quad \mathbf{E}_{\mu,d}^F(t) = \mathbf{D}\mathbf{P}_q^F(t) + \mathbf{B}\mathbf{P}_q^L(t), \quad (32a)$$

$$\mu \in \{x, y, z\}, \forall t, \quad \mathbf{E}_{q,c}^F = -\mathbf{D}^{-1}\mathbf{E}_{q,d}^F + \mathbf{B}\mathbf{E}_{q,c}^L, \quad (32b)$$

Proof. Let

$$\mu \in \{x, y, z\}, i_j \in \mathcal{V}_F, \quad \mu_{i_j,d} = \sum_{k \in \mathcal{N}_{i_j}} w_{i_j,k} \mu_k,$$

then, row j of relation (32a) can be expressed as follows:

$$\mu_{i_{j+n+1},d} - \mu_{i_{j+n+1}} = -\mu_{i_{j+n+1}} + \sum_{k \in \mathcal{N}_{i_j}} w_{i_j,k} \mu_k,$$

where $\mu \in \{x, y, z\}$, $i_j \in \mathcal{V}_F$. Considering the key property of homogeneous transformation, $\mathbf{B} = -\mathbf{D}\mathbf{W}_L$ and $\mathbf{P}_{\mu,c}^L$, Eq. (32a) can be rewritten as

$$\mathbf{E}_{\mu,d}^F = \mathbf{D} \left(\mathbf{P}_{\mu}^F - \mathbf{W}_L \underbrace{\left(\mathbf{P}_{\mu,c}^L - \mathbf{E}_{\mu,c}^L \right)}_{\mathbf{P}_{\mu}^L} \right) = \mathbf{D} \left(-\mathbf{E}_{\mu,c}^F - \mathbf{B}\mathbf{E}_{\mu,c}^L \right).$$

where $\mu \in \{x, y\}$. Therefore, $\mathbf{E}_{\mu,c}^F = -\mathbf{D}^{-1}\mathbf{E}_{\mu,d}^F + \mathbf{B}\mathbf{E}_{\mu,c}^L$. \square

Theorem 1. Assume control inputs \mathbf{U}_L and \mathbf{U}_F are designed so that

$$\forall j \in \mathcal{V}, \forall \mu \in \{x, y, z\}, \quad |\mu_j - \mu_{j,d}| \leq \Delta_\mu, \quad (33)$$

where μ_j and $\mu_{j,d} = \sum_{h \in \mathcal{N}_j} w_{j,h} \mu_h$ are components $\mu \in \{x, y, z\}$ of the actual and local desired positions of vehicle

i ; communication weight $w_{j,h}$ is obtained using Eq. (24). Then,

$$\sqrt{(x_j - x_{j,c})^2 + (y_j - y_{j,c})^2 + (z_j - z_{j,c})^2} \leq \Delta, \quad (34)$$

where

$$\Delta = \Xi_{\max} \sqrt{\Delta_x^2 + \Delta_y^2 + \Delta_z^2}, \quad (35a)$$

$$\Xi_{\max} = \max_l \left(- \sum_{j=1}^{N-n-1} \mathbf{D}_{lj}^{-1} + \sum_{j=1}^{n+1} \mathbf{B}_{lj} \right) \quad (35b)$$

Considering Eq. (32b), we can write

$$\begin{aligned} |\mu_{i_j,c} - \mu_{i_j}| &= \left| - \sum_{j=1}^{N-n-1} D_{lj}^{-1} (\mu_{i_{j+n+1},c} - \mu_{i_{j+n+1}}) + \right. \\ &\quad \left. \sum_{j=1}^{n+1} B_{lj} (\mu_{i_j,c} - \mu_{i_j}) \right| \leq - \sum_{j=1}^{N-n-1} D_{lj}^{-1} |\mu_{i_{j+n+1},c} - \mu_{i_{j+n+1}}| + \\ &\quad \sum_{j=1}^{n+1} B_{lj} |q_{i_j,c} - q_{i_j}| \leq - \sum_{j=1}^{N-n-1} D_{lj}^{-1} \Delta_\mu + \sum_{j=1}^{n+1} B_{lj} \Delta_\mu \\ &\leq \Delta_\mu \max_l \left(- \sum_{j=1}^{N-n-1} \mathbf{D}_{lj}^{-1} + \sum_{j=1}^{n+1} \mathbf{B}_{lj} \right) = \Xi_{\max} \Delta_\mu \end{aligned}$$

for $\mu \in \{x, y, z\}$. Therefore, inequality (34) is satisfied. \square

Theorem 1 specifies an upper limit for deviation of actual position of vehicle i from the desired coordination defined at HDM. It is assumed that every vehicle is enclosed by a vertical cylinder of radius ϵ , and d_{min} denotes the minimum separation distance between every vehicle pair in the reference configuration. Then, inter-agent collision avoidance is guaranteed in a homogeneous deformation coordination, if the following inequality constraint is satisfied at any time t [20]:

$$\forall t, \quad \min\{\sigma_1(t), \sigma_2(t), \sigma_3(t)\} \geq \frac{\Delta + \epsilon}{\frac{d_{min}}{2} + \epsilon}. \quad (36)$$

4.1.5 HDM Control System

It is assumed that vehicle $j \in \mathcal{V}$ has a nonlinear dynamics given by

$$\begin{cases} \dot{\mathbf{x}}_j = \mathbf{f}_j(\mathbf{x}_j, \mathbf{u}_j) \\ \mathbf{r}_j = [x_j \ y_j \ z_j]^T \end{cases}, \quad (37)$$

where $\mathbf{x}_j \in \mathbb{R}^{n_{\mathbf{x},j} \times 1}$ and $\mathbf{u}_j \in \mathbb{R}^{n_{\mathbf{u},j} \times 1}$ are the state and input vectors, and $\mathbf{r}_j = [x_j \ y_j \ z_j]^T$ is the actual position of vehicle j considered as the output of vehicle j .

As aforementioned, leaders move independently at the HDM. Therefore, $\mathcal{N}_i = \emptyset$, if $i \in \mathcal{V}_L$. Dynamics of the vehicle team is given by:

$$\text{Leaders : } \begin{cases} \dot{\mathbf{X}}_L = \mathbf{F}_L(\mathbf{X}_L, \mathbf{U}_L) \\ \mathbf{R}_L = \text{vec}\left([\mathbf{r}_{i_1} \cdots \mathbf{r}_{i_{n+1}}]^T\right) \end{cases}$$

$$\text{Followers : } \begin{cases} \dot{\mathbf{X}}_F = \mathbf{F}_F(\mathbf{X}_F, \mathbf{U}_F) \\ \mathbf{R}_F = \text{vec}\left([\mathbf{r}_{i_{n+2}} \cdots \mathbf{r}_{i_N}]^T\right) \end{cases}$$

where $\text{vec}(\cdot)$ vectorizes matrix $[\cdot]$, \mathbf{X}_F and \mathbf{X}_L are the state vectors representing leaders and followers, respectively, \mathbf{U}_F and \mathbf{U}_L are the leaders' and followers' control inputs. $\mathbf{F}_L = [\mathbf{f}_{i_1}^T \cdots \mathbf{f}_{i_{n+1}}^T]^T$ and $\mathbf{F}_F = [\mathbf{f}_{i_{n+2}}^T \cdots \mathbf{f}_{i_N}^T]^T$ are smooth functions where \mathbf{f}_{i_k} ($k = 1, \dots, N_F$) specifies the dynamics of vehicle i_k previously given in (37). Also, $\mathbf{R}_L = \text{vec}\left([\mathbf{r}_{i_1} \cdots \mathbf{r}_{i_{N_L}}]^T\right)$ and $\mathbf{R}_F = \text{vec}\left([\mathbf{r}_{i_{N_L+1}} \cdots \mathbf{r}_{i_N}]^T\right)$ where $\mathbf{r}_{i_k} = [x_{i_k} \ y_{i_k} \ z_{i_k}]$ denotes actual position of vehicle i_k ($k = 1, \dots, N_F$), $\mathbf{X}_L = [\mathbf{x}_{i_1}^T \cdots \mathbf{x}_{i_{n+1}}^T]^T$, $\mathbf{U}_L = [\mathbf{u}_{i_1}^T \cdots \mathbf{u}_{i_{n+1}}^T]^T$, $\mathbf{X}_F = [\mathbf{x}_{i_{n+2}}^T \cdots \mathbf{x}_{i_N}^T]^T$, and $\mathbf{U}_L = [\mathbf{u}_{i_{n+2}}^T \cdots \mathbf{u}_{i_N}^T]^T$. Fig. 3

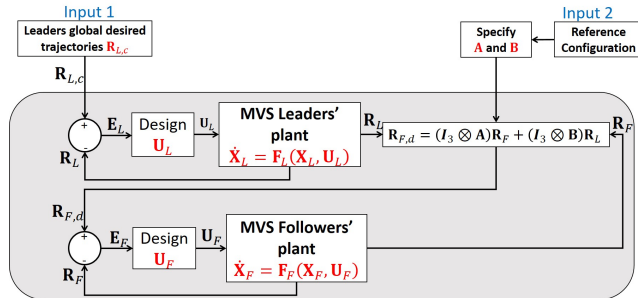


Figure 3. Functionality of the cooperative team when HDM is active.

shows the functionality of the cooperative control system in HDM. As shown the system has the following inputs:

- (1) Global desired trajectories of all leaders specified by vector $\mathbf{R}_L(t)$ at any time t .
- (2) Matrix \mathbf{A} and \mathbf{B} assigned based on the cooperative team reference configuration using relation (27).

Leader global desired trajectories can be safely planned so that collision with obstacles and inter-agent collision are both avoided while the leaders' distances between initial and target states are minimized. Leader path planning using A* search and particle swarm optimization were previously studied in Refs. [13, 21]. Control inputs \mathbf{U}_L and \mathbf{U}_F can be assigned using existing approaches so the actual trajectory \mathbf{r}_j is asymptotically tracked $\mathbf{r}_{j,c}$ for every vehicle $j \in \mathcal{V}$; specific analysis of tracking is beyond the scope of this paper.

4.2 Containment Exclusion Mode (CEM)

CEM is activated when there exists at least one vehicle experiencing a failure or anomaly in containment domain Ω_{con} . Failed agent(s) are wrapped with an exclusion zone and healthy agents must be routed or "flow" around. Thus, $N_F(t) < N(t)$ and $|\mathcal{V}_A(t)| > 0$ at any time t when CEM is active. For CEM, the coordinate transformation defined in (18) is used to assign the desired agent coordination. In particular, potential function ϕ and stream function ψ are determined by combining "Uniform" and "Doublet" flows:

$$\begin{aligned} \phi(x, y, t) &= \phi_U(x, y, t) + \phi_D(x, y, t) \\ \psi(x, y, t) &= \psi_U(x, y, t) + \psi_D(x, y, t) \end{aligned}$$

where the subscripts U and D are associated with "Uniform" and "Doublet", respectively. For the uniform flow pattern,

$$\phi_U(x, y, t) = u_\infty(t)(x \cos \theta_\infty(t) + y \sin \theta_\infty(t)) \quad (38a)$$

$$\psi_U(x, y, t) = u_\infty(t)(-x \sin \theta_\infty(t) + y \cos \theta_\infty(t)), \quad (38b)$$

define the potential and stream fields, respectively, where $u_\infty(t)$ and $\theta_\infty(t)$ are design parameters. Furthermore,

$$\phi_D = \sum_{i \in \mathcal{V}_A} \phi_{D,i} \quad \text{and} \quad \psi_D = \sum_{i \in \mathcal{V}_A} \psi_{D,i},$$

define potential and stream fields of the Doublet flow, respectively, where

$$\phi_{D,i} = \frac{\delta_i(t)[\cos \gamma_i(t)(x - a_i(t)) + \sin \gamma_i(t)(y - b_i(t))]}{(x - a_i(t))^2 + (y - b_i(t))^2}, \quad (39a)$$

$$\psi_{D,i} = \frac{\delta_i(t)[- \sin \gamma_i(t)(x - a_i(t)) + \cos \gamma_i(t)(y - b_i(t))]}{(x - a_i(t))^2 + (y - b_i(t))^2}, \quad (39b)$$

and Δ_i , a_i , b_i are design parameters specifying the geometry and location of anomalous/failed agent $i \in \mathcal{V}_A$ in the motion space. By treating agent coordination as ideal fluid flow, we can exclude failed agent $i \in \mathcal{V}_A$ by wrapping them with a closed surface $\psi(x, y, t) = \psi_{i,0}$, where $\psi_{i,0}$ is constant. Furthermore, healthy vehicle $j \in \mathcal{V}_H$ moves along the global desired trajectories

$$\psi_{j,c}(t) = \psi(x_{j,c}(t), y_{j,c}(t), t) = \psi_{j,0} \text{ (constant)}. \quad (40)$$

where $\psi_{j,0}$ is assigned based on position of vehicle $j \in \mathcal{V}_H$ at the time the cooperative team enters the CEM.

Theorem 2. Suppose $\mathbf{J}(x_j, y_j)$ is the Jacobian matrix defined by (21), and the desired trajectory of every agent

$j \in \mathcal{V}_H$ satisfies Eq. (20). Define

$$\mathbf{H}_{s,j} = -\frac{1}{|\mathbf{J}(x_j, y_j)|} \begin{bmatrix} \frac{\partial \psi}{\partial y_{j,c}} \\ -\frac{\partial y_{j,c}}{\partial \psi} \end{bmatrix} \begin{bmatrix} \frac{\partial \phi}{\partial u_\infty} & \frac{\partial \phi}{\partial \theta_\infty} \end{bmatrix} \quad (41a)$$

$$\mathbf{H}_{a,j,i_l} = -\frac{1}{|\mathbf{J}(x_j, y_j)|} \begin{bmatrix} \frac{\partial \psi}{\partial y_{j,c}} \\ -\frac{\partial y_{j,c}}{\partial \psi} \end{bmatrix} \begin{bmatrix} \frac{\partial \phi}{\partial a_{i_l}} & \frac{\partial \phi}{\partial b_{i_l}} & \frac{\partial \phi}{\partial \Delta_{i_l}} \end{bmatrix}, \quad l = N_F + 1, \dots, N, \quad (41b)$$

$$\mathbf{H}_{T,j} = \frac{1}{|\mathbf{J}(x_j, y_j)|} \begin{bmatrix} \frac{\partial \psi}{\partial y_{j,c}} \\ -\frac{\partial y_{j,c}}{\partial \psi} \end{bmatrix}, \quad (41c)$$

$$\dot{\mathbf{q}}_{c, \text{CEM}} = \begin{bmatrix} \dot{u}_\infty & \dot{\theta}_\infty \end{bmatrix}^T, \quad (41d)$$

$$\dot{\mathbf{q}}_{u, \text{CEM}} = \begin{bmatrix} \dot{a}_{i_{N_F+1}} & \dot{b}_{i_{N_F+1}} & \dot{\Delta}_{i_{N_F+1}} & \cdots & \dot{a}_{i_N} & \dot{b}_{i_N} & \dot{\Delta}_{i_N} \end{bmatrix}^T, \quad (41e)$$

Then, the CEM global desired trajectory can be defined by Eq. (17), where $\gamma = \text{CEM}$,

$$\dot{\mathbf{q}}_{\text{CEM}} = \begin{bmatrix} \dot{\mathbf{q}}_{c, \text{CEM}} \\ \dot{\mathbf{q}}_{u, \text{CEM}} \\ v_\phi \end{bmatrix} \in \mathbb{R}^{3+3(N-N_F) \times 1}, \quad (42a)$$

$$\mathbf{H}_{j, \text{CEM}} = \begin{bmatrix} 1 & 0 \\ 0 & 1 \\ \frac{\partial z_{j,c}}{\partial x_{j,c}} & \frac{\partial z_{j,c}}{\partial y_{j,c}} \end{bmatrix} \left[\mathbf{H}_s \ \mathbf{H}_{a,i_{N_F+1}} \ \cdots \ \mathbf{H}_{a,i_N} \ \mathbf{H}_{T,j} \right] \quad (42b)$$

for every agent $j \in \mathcal{V}_H$, where $v_\phi = \frac{\partial \phi}{\partial t}$ is the desired sliding speed of healthy vehicles along their desired stream lines.

Proof. Per the prescribed CEM protocol vehicle i slides along the stream line $\psi_{j,c} = \psi_{j,0}$ at any time t . Eq. (20) must be satisfied at every point $(x_{j,c}, y_{j,c})$ and any time t . Given the sliding speed v_ϕ , the following relation holds:

$$\begin{aligned} \frac{\partial \phi}{\partial x_{j,c}} \dot{x}_{j,c} + \frac{\partial \phi}{\partial y_{j,c}} \dot{y}_{j,c} &= -\frac{\partial \phi}{\partial u_\infty} \dot{u}_\infty - \frac{\partial \phi}{\partial \theta_\infty} \dot{\theta}_\infty \\ &- \sum_{i \in \mathcal{V}_A} \left(\frac{\partial \phi}{\partial a_i} \dot{a}_i + \frac{\partial \phi}{\partial b_i} \dot{b}_i + \frac{\partial \phi}{\partial \Delta_i} \dot{\Delta}_i \right) + v_\phi, \end{aligned} \quad (43a)$$

$$\frac{\partial \psi}{\partial x_{j,c}} \dot{x}_{j,c} + \frac{\partial \psi}{\partial y_{j,c}} \dot{y}_{j,c} = 0. \quad (43b)$$

Therefore, x and y components of agent $j \in \mathcal{V}_H$ global desired trajectory are updated by (17), where $\mathbf{H}_{j, \text{CEM}}$ and $\dot{\mathbf{q}}_{\text{CEM}}$ are given by Eq. (42) for agent $j \in \mathcal{V}_H$ at any time t . \square

Design parameters $\dot{u}_\infty, \dot{\theta}_\infty, \dot{\Delta}_i, \dot{a}_i, \dot{b}_i$ ($i \in \mathcal{V}_A$), and v_ϕ , obtained by taking time derivative from the generalized coordinates, define group desired coordination for CEM. Note that u_∞ and θ_∞ can be designed so that the ideal fluid flow coordination is optimized. However, the remaining design parameters are uncontrolled.

Remark 1. In general, design parameters $\dot{u}_\infty, \dot{\theta}_\infty, \dot{\Delta}_i, \dot{a}_i, \dot{b}_i$ ($i \in \mathcal{V}_A$) can vary with time. However, this paper concentrates only on the steady-state CEM which will be achieved when $\dot{u}_\infty, \dot{\theta}_\infty, \dot{\Delta}_i, \dot{a}_i, \dot{b}_i$ ($i \in \mathcal{V}_A$) are all zeros. Therefore, potential and stream functions are defined by Eqs. (38), and (39) simplifies to

$$j \in \mathcal{V}_H, \quad \begin{bmatrix} \dot{x}_{j,c} \\ \dot{y}_{j,c} \\ \dot{z}_{j,c} \end{bmatrix} = \begin{bmatrix} 1 & 0 \\ 0 & 1 \\ \frac{\partial z_{j,c}}{\partial x_{j,c}} & \frac{\partial z_{j,c}}{\partial y_{j,c}} \end{bmatrix} \mathbf{H}_{T,j} v_\phi.$$

This requires an assumption for this work that the failed vehicle $i \in \mathcal{V}_A$ remains inside a predictable closed domain, with time-invariant geometry, until the time the failed agent is no longer in containment domain Ω_{con} defined per Eq. (13).

5 Continuum Deformation Anomaly Management

This section develops a hybrid model to manage transitions between CEM and HDM. Section 5.1 develops a distributed approach to detect a vehicle failure/anomaly followed by a supervisory control transition approach described in Section 5.2.

5.1 Anomaly Detection

In this sub-section, we present a distributed model to detect situations in which agents have failed or are no longer cooperative. We then consider these agents anomalous or failed and add them to anomalous agent set \mathcal{V}_A .

Consider an n -D homogeneous deformation where follower i knows its own position and positions of in-neighbor agents $\mathcal{N}_i = \{j_1, \dots, j_{n+1}\}$ at any time t . Let actual position $\mathbf{r}_i(t)$ be expressed as the convex combination of agent i 's in-neighbors by

$$i \in \mathcal{V}_F, \quad \mathbf{r}_i(t) = \sum_{k=1}^{n+1} \varpi_{i,j_k}(t) \mathbf{r}_{j_k}. \quad (44a)$$

$$i \in \mathcal{V}_F, \quad \sum_{k=1}^{n+1} \varpi_{i,j_k}(t) = 1, \quad (44b)$$

where ϖ_{i,j_1} through $\varpi_{i,j_{n+1}}$ are called *transient weights*. If $\chi_n(\mathbf{r}_{j_1}(t), \dots, \mathbf{r}_{j_{n+1}}(t)) = n$, transient weights ϖ_{i,j_1}

through $\varpi_{i,j_{n+1}}$ can be assigned based on agents' actual positions as follows:

$$\left[\varpi_{i,j_1}(t) \cdots \varpi_{i,j_4}(t) \right]^T = \Lambda \left(\mathbf{r}_{j_1}, \mathbf{r}_{j_2}, \mathbf{r}_{j_3}, \mathbf{r}_{j_4}^n, \mathbf{r}_i^n \right), \quad (45)$$

where

$$\mathbf{r}_{j_4}^n(t) = \begin{cases} \mathbf{r}_{j_4}(t) & n=3 \\ \mathbf{r}_{j_1} + \Xi(\mathbf{r}_{j_3,0} - \mathbf{r}_{j_1,0}) \times (\mathbf{r}_{j_2,0} - \mathbf{p}_{j_1,0}) & n=2 \end{cases}, \quad (46a)$$

$$\mathbf{r}_{i,0}^n(t) = \begin{cases} \mathbf{r}_i & n=3 \\ \mathbf{r}_i - (\mathbf{r}_i \cdot \mathbf{n}_{1-4}) \mathbf{n}_{1-4} & n=2 \end{cases}, \quad (46b)$$

$$\Gamma_3(\mathbf{r}_{j_1}(t), \mathbf{r}_{j_2}(t), \mathbf{r}_{j_3}(t), \mathbf{r}_{j_4}(t)) = 3. \quad (47)$$

and $\mathbf{n}_{1-4} = \mathbf{n}_{1-4}(\mathbf{r}_{j_1}, \mathbf{r}_{j_2}, \mathbf{r}_{j_3})$ is determined based on agents' actual positions using Eq. (6) when $n=2$.

Geometric Interpretation of Transient Weights:

Let $d_{i,j_2,j_3}(t)$, $d_{i,j_3,j_1}(t)$, and $d_{i,j_1,j_2}(t)$ denote distances of point i from the triangle sides j_2-j_3 , j_3-j_1 , and j_1-j_2 , respectively. Assume $l_{j_1,j_2,j_3}(t)$, $l_{j_2,j_3,j_1}(t)$, $l_{j_3,j_1,j_2}(t)$ determine distances of vertices j_1 , j_2 , and j_3 from the triangle sides j_2-j_3 , j_3-j_1 , j_1-j_2 , respectively. Then,

$$\varpi_{i,j_1}(t) = \frac{d_{i,j_2,j_3}}{l_{j_1,j_2,j_3}}, \quad (48a)$$

$$\varpi_{i,j_2}(t) = \frac{d_{i,j_3,j_1}}{l_{j_2,j_3,j_1}}, \quad (48b)$$

$$\varpi_{i,j_3}(t) = \frac{d_{i,j_1,j_2}}{l_{j_3,j_1,j_2}}. \quad (48c)$$

Geometric representations of $d_{i,j_2,j_3}(t)$ and $l_{j_1,j_2,j_3}(t)$ are shown in Fig. 4 (a) when $n=2$.

For $n=3$, $d_{i,j_2,j_3,j_4}(t)$, $d_{i,j_3,j_4,j_1}(t)$, $d_{i,j_4,j_1,j_2}(t)$, and $d_{i,j_1,j_2,j_3}(t)$ denote distance of point i from the triangular surfaces $j_2-j_3-j_4$, $j_3-j_4-j_1$, $j_4-j_1-j_2$, $j_1-j_2-j_3$, respectively. Assume $l_{j_1,j_2,j_3,j_4}(t)$, $l_{j_2,j_3,j_4,j_1}(t)$, $l_{j_3,j_4,j_1,j_2}(t)$, and l_{j_4,j_1,j_2,j_3} determine distance of vertices j_1 , j_2 , j_3 , and j_4 , from the triangular surfaces $j_2-j_3-j_4$, $j_3-j_4-j_1$, $j_4-j_1-j_2$, and $j_1-j_2-j_3$ respectively. Then,

$$\varpi_{i,j_1}(t) = \frac{d_{i,j_2,j_3,j_4}}{l_{j_1,j_2,j_3,j_4}}, \quad (49a)$$

$$\varpi_{i,j_2}(t) = \frac{d_{i,j_3,j_4,j_1}}{l_{j_2,j_3,j_4,j_1}(t)}, \quad (49b)$$

$$\varpi_{i,j_3}(t) = \frac{d_{i,j_4,j_1,j_2}}{l_{j_3,j_4,j_1,j_2}(t)}, \quad (49c)$$

$$\varpi_{i,j_4}(t) = \frac{d_{i,j_4,j_1,j_2}}{l_{j_3,j_4,j_1,j_2}(t)}. \quad (49d)$$

Theorem 3. Assume HDM collective motion is guided by $n+1$ leaders, defined by \mathcal{V}_L , every follower $i \in \mathcal{V}_F$, communicates with $n+1$ in-neighbor agents, defined by $\mathcal{N}_i = \{j_1, \dots, j_{n+1}\}$, where follower i 's in-neighbors form an n -D simplex at time t . If deviation of every agent $i \in \mathcal{V}$ from the global desired position $\mathbf{r}_{i,c}$ is less than Δ at time t ($|\mathbf{r}_i(t) - \mathbf{r}_{i,c}(t)| \leq \Delta$), then followers' communication weights satisfy the following inequality:

$$\varpi_{i,j_1}^{\min}(t) \leq w_{i,j_1} \leq \varpi_{i,j_1}^{\max}(t), \quad (50)$$

where $w_{i,j}$ is constant communication weight of follower $i \in \mathcal{V}$ with in-neighbor j_1 assigned by Eq. (24), and

$$\varpi_{i,j_1}^{\min}(t) = \begin{cases} \frac{d_{i,j_2,j_3}(t) - \Delta}{l_{j_1,j_2,j_3}(t) + 2\Delta} & n=2 \\ \frac{d_{i,j_2,j_3,j_4}(t) - \Delta}{l_{j_1,j_2,j_3,j_4} + 2\Delta} & n=3 \end{cases}, \quad (51a)$$

$$\varpi_{i,j_1}^{\max}(t) = \begin{cases} \frac{d_{i,j_2,j_3,j_4}(t) + 2\Delta}{l_{j_1,j_2,j_3}(t) - \Delta} & n=2 \\ \frac{d_{i,j_2,j_3,j_4}(t) + 2\Delta}{l_{j_1,j_2,j_3,j_4} - \Delta} & n=3 \end{cases}. \quad (51b)$$

specify lower and upper bounds for transient weight $\varpi_{i,j_1}(t)$ at time t .

Proof. If $\mathbf{r}_i(t) = \mathbf{r}_{i,c}(t)$ for every agent $i \in \mathcal{V}$ at any time t , then $\varpi_{i,j_k}(t) = w_{i,j_k}$ ($k=1, \dots, n+1, j_k \in \mathcal{N}_i$). For $n=2$, we define a desired triangle $j_1-j_2-j_3$ with vertices placed at $\mathbf{r}_{j_1,c}$, $\mathbf{r}_{j_2,c}$, and $\mathbf{r}_{j_3,c}$. D_{i,j_2,j_3} denotes the distance between the global desired position of agent i and the triangle side j_2-j_3 while L_{j_1,j_2,j_3} denotes the distance between the desired position of agent j_1 and the side j_2-j_3 of the desired tetrahedron. We also define an "actual" triangle with vertices positioned at \mathbf{r}_{j_1} , \mathbf{r}_{j_2} , and \mathbf{r}_{j_3} . When $\|\mathbf{r}_i(t) - \mathbf{r}_{i,c}(t)\| \leq \Delta$ is satisfied for agent $i \in \mathcal{V}$, then,

$$d_{i,j_2,j_3}(t) - 2\Delta \leq D_{i,j_2,j_3}(t) \leq d_{i,j_2,j_3}(t) + 2\Delta, \quad (52a)$$

$$l_{i,j_2,j_3}(t) - 2\Delta \leq L_{i,j_2,j_3}(t) \leq l_{i,j_2,j_3}(t) + 2\Delta. \quad (52b)$$

$$\text{Therefore, } w_{i,j_1} = \frac{D_{i,j_2,j_3}(t)}{L_{i,j_2,j_3}(t)} \in \left[\frac{d_{i,j_2,j_3} - 2\Delta}{L_{i,j_2,j_3} + 2\Delta}, \frac{d_{i,j_2,j_3} + 2\Delta}{L_{i,j_2,j_3} - 2\Delta} \right]$$

(See Fig. 4). For $n=3$, vertices of the desired tetrahedron $j_1-j_2-j_3-j_4$ are placed at $\mathbf{r}_{j_1,c}$, $\mathbf{r}_{j_2,c}$, $\mathbf{r}_{j_3,c}$, and $\mathbf{r}_{j_4,c}$; vertices of the "actual" tetrahedron are positioned at \mathbf{r}_{j_1} , \mathbf{r}_{j_2} , \mathbf{r}_{j_3} , and \mathbf{r}_{j_4} . D_{i,j_1,j_2,j_3} denotes the distance between the global desired position of agent i and the tetrahedron surface $j_2-j_3-j_4$. L_{j_1,j_2,j_3} denotes the distance between the desired position of agent j and the surface $j_2-j_3-j_4$ of the desired tetrahedron. Assuming every agent $i \in \mathcal{V}$ satisfies safety constraint (34),

$$d_{i,j_2,j_3,j_4}(t) - 2\Delta \leq D_{i,j_2,j_3,j_4}(t) \leq d_{i,j_2,j_3,j_4}(t) + 2\Delta, \quad (53a)$$

$$l_{i,j_2,j_3,j_4}(t) - 2\Delta \leq L_{i,j_2,j_3,j_4}(t) \leq l_{i,j_2,j_3,j_4}(t) + 2\Delta, \quad (53b)$$

Therefore,

$$w_{i,j_1} = \frac{D_{i,j_2,j_3,j_4}(t)}{L_{i,j_2,j_3,j_4}(t)} \in \left[\frac{d_{i,j_2,j_3,j_4} - 2\Delta}{L_{i,j_2,j_3,j_4} + 2\Delta}, \frac{d_{i,j_2,j_3,j_4} + 2\Delta}{L_{i,j_2,j_3,j_4} - 2\Delta} \right].$$

□

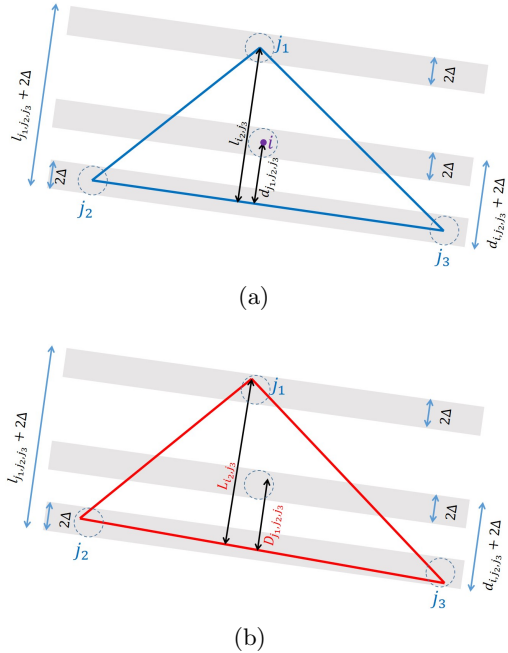


Figure 4. (a) “Actual” triangle constructed by the actual positions of agents j_1 , j_2 , and j_3 at time t . (b) Desired triangle given by the global desired positions of agents j_1 , j_2 , and j_3 at time t .

Theorem 3 implies that HDM mode is active only if the following condition is satisfied:

$$\forall i \in \mathcal{V}, k = 1, \dots, n+1, \quad \varpi_{i,j_k}^{\min}(t) \leq w_{i,j_k} \leq \varpi_{i,j_k}^{\max}(t), \quad (\Psi_{i,j_k})$$

where $\mathcal{N}_i = \{j_1, \dots, j_{n+1}\}$ defines in-neighbors of agent $i \in \mathcal{V}$. Therefore, if $\bigwedge_{i=1}^{N(t)} \bigwedge_{k=1}^{n+1} \Psi_{i,j_k}$ is satisfied at time t , HDM is active. Otherwise, an anomaly is detected. Additionally, disjoint sets \mathcal{V}_H and \mathcal{V}_A are defined as follows:

$$\mathcal{V}_H(t) = \left\{ j \in \mathcal{V}(t) \mid \bigwedge_{h \in \mathcal{N}_h} \Psi_{i,j_h} \text{ is satisfied.} \right\}, \quad (54a)$$

$$\mathcal{V}_A(t) = \mathcal{V}(t) \setminus \mathcal{V}_H(t). \quad (54b)$$

5.2 Vehicle Anomaly/Failure Management

The Fig. 5 flowchart illustrates how vehicle failure can be managed by transition between “HDM” and “CEM”. The following procedure is proposed:

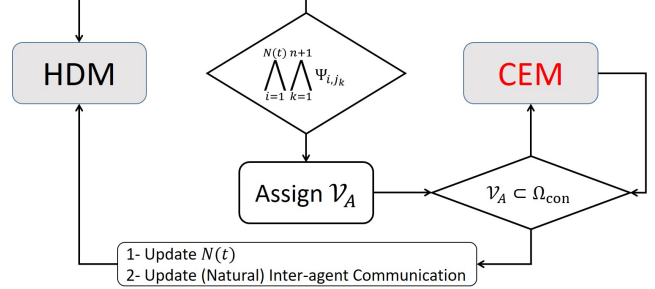


Figure 5. Failed vehicle assignment and management by cooperative team leaders.

- (1) Define containment domain $\Omega_{\text{con}}(\mathbf{r}, \mathbf{r}_{\text{con}}(t))$ using Eq. (13).
- (2) If there exists at least one failed agent inside the containment domain $\Omega_{\text{con}}(\mathbf{r}, \mathbf{r}_{\text{con}}(t))$, then

$$\bigwedge_{i=1}^{N(t)} \bigwedge_{k=1}^{n+1} \Psi_{i,j_k}$$

- is **not** satisfied and CEM is activated.
- (3) If agents contained by $\Omega_{\text{con}}(\mathbf{r}, \mathbf{r}_{\text{con}}(t))$ are all healthy, then $\bigwedge_{i=1}^{N(t)} \bigwedge_{k=1}^{n+1} \Psi_{i,j_k}$ is **satisfied** which in turn implies that $\mathcal{V}_A = \emptyset$ and HDM is active.

6 Simulation Results

Consider collective motion in a 2-D plane with invariant z components for all agents at all times t . Suppose a multi-agent team consisting of 22 vehicles is deployed with the initial formation shown in Fig. 2. Given global desired positions of all agents at time t , the containment domain Ω_{com} is defined for this case study as:

$$\Omega_{\text{con}} = \|\mathbf{r} - \mathbf{r}_{\text{con}}\|_1 \leq 40,$$

where $\mathbf{r}_{\text{con}} = \frac{1}{N(t)} \sum_{i \in \mathcal{V}_H} \mathbf{r}_i$ and $\|\cdot\|_1$ denotes the 1-norm. Therefore, Ω_{con} is a box with side length 80m.

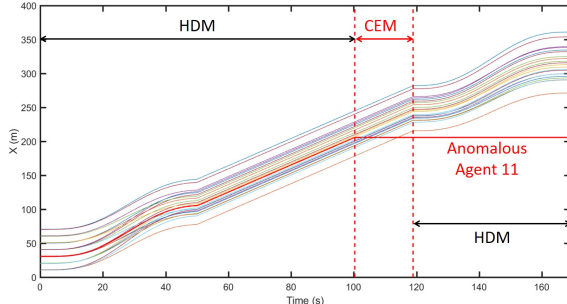
Without loss of generality, assume that every agent is a single integrator. The position of each agent i is updated by

$$i \in \mathcal{V}, \quad \dot{\mathbf{r}}_i = g(\mathbf{r}_{i,d} - \mathbf{r}_i), \quad (55)$$

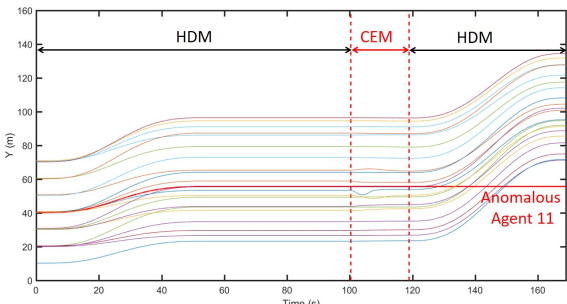
where $g = 25$ is constant, \mathbf{r}_i is the actual position of agent i , and local desired position $\mathbf{r}_{i,d}$ was defined in Eq. (28).

6.1 Motion Phase 1 (HDM)

Team collective motion is defined by a homogeneous transformation over $t \in [0, 100]$, where agents are all healthy. Agents $i_1 = 1$, $i_2 = 2$, and $i_3 = 3$ are the leaders defining the homogeneous transformation. Given leaders’ desired trajectories, eigenvalues of the desired homogeneous deformation coordination, denoted by σ_1 and



(a)



(b)

Figure 6. (a,b) x and y components of actual positions of agents versus time for $t \in [0, 168.91]s$. HDM is initially active over $t \in [0, 100]s$. Agent 11 is flagged anomalous at time $t \in [100, 100.35]s$ thus CEM is activated. At $t = 118.92s$, agent 11 is no longer inside the containment box Ω_{con} . Therefore, HDM is activated.

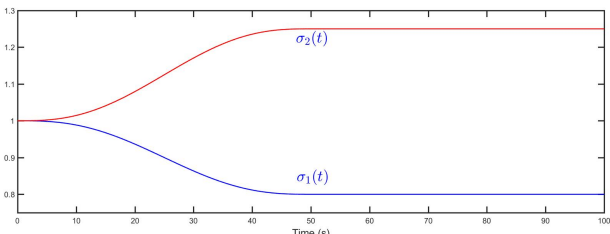


Figure 7. Homogeneous deformation eigenvalues σ_1 and σ_2 versus time for $t \in [0, 100]s$.

σ_2 , are plotted versus time in Fig. 7. Note that $\sigma_3(t) = 1$ at any time t because agents are treated as particles of a 2-D continuum and the desired homogenous deformation coordination is also two dimensional. Follower vehicles apply the communication graph shown in Fig. 2 to acquire the desired coordination by local communication. The communication graph is strictly 3-reachable per Section 4.1. Given initial positions of all agents, every follower chooses three in-neighbor agents using the approach described in Section 4.1. Consequently, the graph shown in Fig. 4.1 assigns inter-agent communication, where followers' communication weights are consistent with agents' positions at reference time $t = 0$ and obtained by (24). As shown Fig. 4, HDM is active before an anomaly situation arises at time $t = 100s$.

6.2 Motion Phase 2 (CEM)

Suppose agent 11 fails at time $t = 100$. This failure is quickly detected by the team using the distributed failure detection method developed in Section 5. As shown in Figs. 8 (a),(c),(d), conditions $\varpi_{11,13}^{\min}(t) \leq w_{11,13} \leq \varpi_{11,13}^{\max}(t)$, $\varpi_{11,8}^{\min}(t) \leq w_{11,8} \leq \varpi_{11,8}^{\max}(t)$, and $\varpi_{11,6}^{\min}(t) \leq w_{11,6} \leq \varpi_{11,6}^{\max}(t)$ ϖ_{11} are satisfied over $t \in [0, 100]s$. However, condition $\varpi_{11,6}^{\min}(t) \leq w_{11,6} \leq \varpi_{11,6}^{\max}(t)$ is violated at $t = 100.34$ when $\varpi_{11,6}^{\min}(100.34) > w_{11,6}$. Therefore, CEM is activated, and healthy agent coordination is treated as an ideal fluid flow after $100.35s$. The ideal fluid flow coordination is defined by combining “Uniform” and “Doublet” flow patterns. Anomalous agent 11 is wrapped by a disk of radius $a = 4m$ resulted from choosing $u_\infty = 10$, and $\delta = 160$, i.e. $a = \sqrt{\frac{\delta}{u_\infty}} = 4m$. The remaining healthy vehicles slide along level curves $\psi_{i,c}(t) = \psi_{i,0}$, where each $\psi_{i,0}$ is determined based on agent i 's position at $t = 100.35s$.

In Fig. 9, actual paths of the healthy agents, defined by $\mathcal{V}_H = \{1, \dots, 10, 12, \dots, 22\}$ are shown for $t \in [100.35, 118.92]$. Green markers show positions of healthy agents at $t = 100.35s$ when they enter CEM; black markers show positions of healthy agents at $t = 118.92s$ when CEM ends. Failed agent 11 is wrapped by a disk of radius $4m$ centered at $(205.26, 55.62)$ in this example.

6.3 Motion Phase 3 (HDM)

CEM continues until switching time $118.92s$ when failed agent 11 leaves containment box Ω_{con} . Fig. 10 shows the agents' configuration at time $t = 118.92$. Followers use the method from Section 4.1 to find their in-neighbors as well as communication weights. HDM remains active after $t = 118.92$ since no other agents fail in this simulation. x and y components of actual agent positions were plotted versus time for $t \in [118.92, 168.92]s$ earlier in Fig. 6.

7 Conclusion

This paper develops a hybrid cooperative control strategy with two operational modes to manage large-scale coordination of agents in a resilient fashion. The first mode (HDM) treats agents as particles of a deformable body and is active when all agents are healthy. HDM guarantees agents can safely initialize and coordinate their motions using the unique features of homogeneous deformation coordination. A new CEM cooperative paradigm was proposed to handle cases in which one or more vehicles in the shared motion space fail to admit the desired coordination. In CEM the desired vehicle coordination is treated as an ideal fluid flow and failed

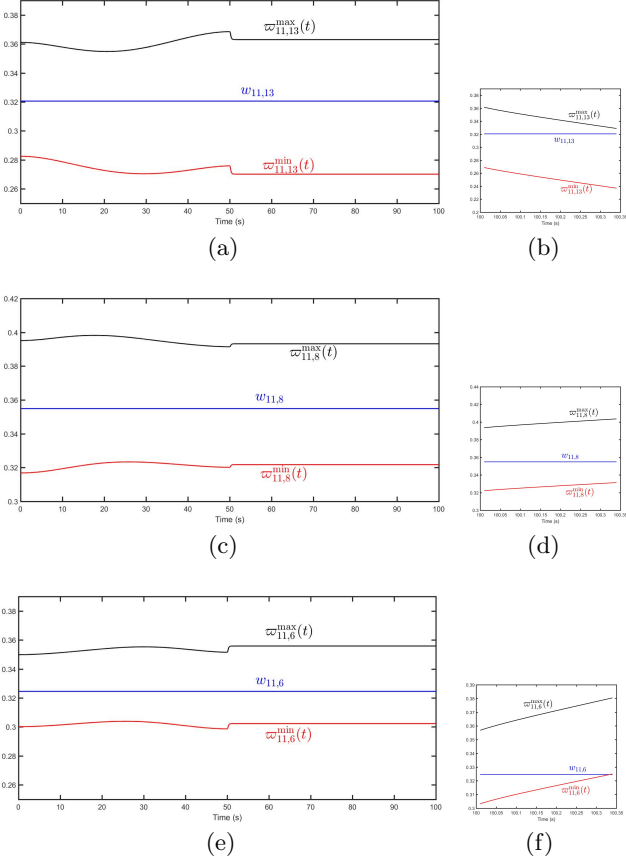


Figure 8. Weights $w_{11,13}$, $\varpi_{11,13}^{\min}(t)$, and $\varpi_{11,13}^{\max}(t)$ for (a) $t \in [0, 100]$ and (b) $t \in [100.01, 100.35]$. Weights $w_{11,8}$, $\varpi_{11,8}^{\min}(t)$, and $\varpi_{11,8}^{\max}(t)$ for (c) $t \in [0, 100]$ and (d) $t \in [100.01, 100.35]$. Weights $w_{11,6}$, $\varpi_{11,6}^{\min}(t)$, and $\varpi_{11,6}^{\max}(t)$ for (e) $t \in [0, 100]$ and (f) $t \in [100.01, 100.35]$. Anomalous motion in agent 11 is detected in 0.34s when $\varpi_{11,6}^{\min}(100.34) > w_{11,6}$.

vehicles are excluded by closed curves. Therefore, desired trajectories for the remaining healthy vehicles can be planned and collective motion safety for healthy vehicles can still be guaranteed with low computation overhead. To automatically initiate transition to CEM, this paper contributes a strategy for quickly detecting agent failure using the unique properties of the homogeneous deformation coordination. Future work is needed to relax motion constraints on failed vehicles and present simulation results with realistic vehicle dynamics and more complex environments.

Acknowledgements

This work has been supported by the National Science Foundation under Award Nos. 1739525 and 1914581.

References

- [1] Rudy Cepeda-Gomez and Nejat Olgac. Exhaustive stability analysis in a consensus system with time delay and irregular

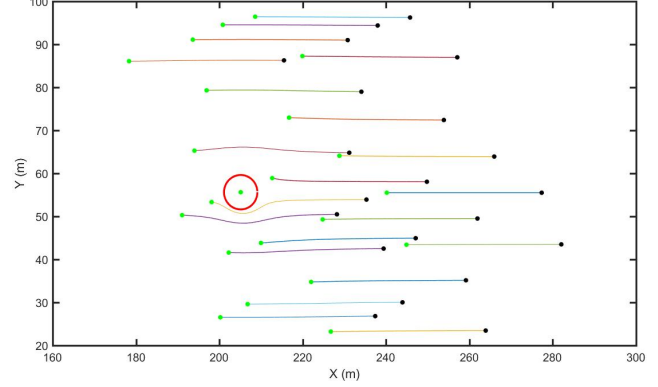


Figure 9. Paths of healthy agents over $t \in [100.35, 118.92]$ when CEM is active. The green and block markers show positions of agents at times 100.35 and 118.92, respectively. Failed agent 11 is wrapped by a disk of radius 4m centered at (205.26, 55.62) when CEM is active.

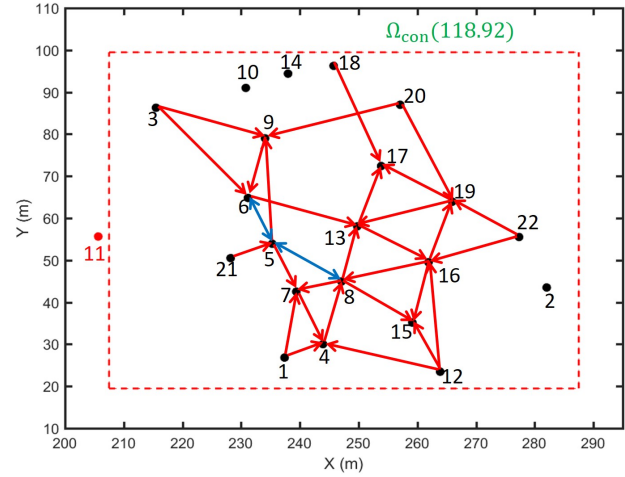


Figure 10. Formation of agents at time $t = 118.92s$. Failed agent 11 is outside the containment region Ω_{con} . HDM is activated and inter-agent communication is established using the procedure developed in Section 4.1.

- topologies. *International Journal of Control*, 84(4):746–757, 2011.
- [2] Teng-Hu Cheng, Zhen Kan, Justin R Klotz, John M Shea, and Warren E Dixon. Event-triggered control of multiagent systems for fixed and time-varying network topologies. *IEEE Transactions on Automatic Control*, 62(10):5365–5371, 2017.
- [3] Michael Defoort, Andrey Polyakov, Guillaume Demesure, Mohamed Djemai, and Kalyana Veluvolu. Leader-follower fixed-time consensus for multi-agent systems with unknown non-linear inherent dynamics. *IET Control Theory & Applications*, 9(14):2165–2170, 2015.
- [4] Seyed Mehran Dibaji and Hideaki Ishii. Resilient consensus of second-order agent networks: Asynchronous update rules with delays. *Automatica*, 81:123–132, 2017.
- [5] Wenyng Hou, Minyue Fu, Huanshui Zhang, and Zongze Wu. Consensus conditions for general second-order multi-agent systems with communication delay. *Automatica*, 75:293–298, 2017.

- [6] Meng Ji, Giancarlo Ferrari-Trecate, Magnus Egerstedt, and Annalisa Buffa. Containment control in mobile networks. *IEEE Transactions on Automatic Control*, 53(8):1972–1975, 2008.
- [7] Jae Man Kim, Jin Bae Park, and Yoon Ho Choi. Leaderless and leader-following consensus for heterogeneous multi-agent systems with random link failures. *IET Control Theory & Applications*, 8(1):51–60, 2014.
- [8] W Michael Lai, David H Rubin, Erhard Krempel, and David Rubin. *Introduction to continuum mechanics*. Butterworth-Heinemann, 2009.
- [9] Heath J LeBlanc. *Resilient cooperative control of networked multi-agent systems*. Vanderbilt University, 2012.
- [10] Heath J LeBlanc, Haotian Zhang, Xenofon Koutsoukos, and Shreyas Sundaram. Resilient asymptotic consensus in robust networks. *IEEE Journal on Selected Areas in Communications*, 31(4):766–781, 2013.
- [11] Wuquan Li, Lihua Xie, and Ji-Feng Zhang. Containment control of leader-following multi-agent systems with markovian switching network topologies and measurement noises. *Automatica*, 51:263–267, 2015.
- [12] Zhiqiang Li, F Richard Yu, and Minyi Huang. A distributed consensus-based cooperative spectrum-sensing scheme in cognitive radios. *IEEE Transactions on Vehicular Technology*, 59(1):383–393, 2009.
- [13] Zihao Liang, Hossein Rastgoftar, and Ella M Atkins. Multi-quadcopter team leader path planning using particle swarm optimization. In *AIAA Aviation 2019 Forum*, page 3258, 2019.
- [14] Peng Lin and Yingmin Jia. Consensus of second-order discrete-time multi-agent systems with nonuniform time-delays and dynamically changing topologies. *Automatica*, 45(9):2154–2158, 2009.
- [15] Xue Lin and Yuanshi Zheng. Finite-time consensus of switched multiagent systems. *IEEE Transactions on Systems, Man, and Cybernetics: Systems*, 47(7):1535–1545, 2016.
- [16] Cheng-Lin Liu and Fei Liu. Stationary consensus of heterogeneous multi-agent systems with bounded communication delays. *Automatica*, 47(9):2130–2133, 2011.
- [17] Huiyang Liu, Guangming Xie, and Long Wang. Necessary and sufficient conditions for containment control of networked multi-agent systems. *Automatica*, 48(7):1415–1422, 2012.
- [18] Nathan Michael, Jonathan Fink, and Vijay Kumar. Cooperative manipulation and transportation with aerial robots. *Autonomous Robots*, 30(1):73–86, 2011.
- [19] Antonis Papachristodoulou, Ali Jadbabaie, and Ulrich Munz. Effects of delay in multi-agent consensus and oscillator synchronization. *IEEE transactions on automatic control*, 55(6):1471–1477, 2010.
- [20] Hossein Rastgoftar. *Continuum deformation of multi-agent systems*. Springer, 2016.
- [21] Hossein Rastgoftar and Ella M Atkins. Multi-uav continuum deformation flight optimization in cluttered urban environments. In *AIAA Scitech 2019 Forum*, page 0914, 2019.
- [22] Hossein Rastgoftar and Suhada Jayasuriya. Evolution of multi-agent systems as continua. *Journal of Dynamic Systems, Measurement, and Control*, 136(4):041014, 2014.
- [23] Hossein Rastgoftar, Jean-Baptiste Jeannin, and Ella Atkins. Formal specification of continuum deformation coordination. In *2019 American Control Conference (ACC)*, pages 3358–3363. IEEE, 2019.
- [24] Wei Ren and Randal Beard. Virtual structure based spacecraft formation control with formation feedback. In *AIAA Guidance, Navigation, and control conference and exhibit*, page 4963, 2002.
- [25] Wei Ren and Randal Beard. Decentralized scheme for spacecraft formation flying via the virtual structure approach. *Journal of Guidance, Control, and Dynamics*, 27(1):73–82, 2004.
- [26] Yilun Shang. Resilient consensus of switched multi-agent systems. *Systems & Control Letters*, 122:12–18, 2018.
- [27] Jun Shen and James Lam. Containment control of multi-agent systems with unbounded communication delays. *International Journal of Systems Science*, 47(9):2048–2057, 2016.
- [28] Housheng Su, Yanyan Ye, Yuan Qiu, Yang Cao, and Michael ZQ Chen. Semi-global output consensus for discrete-time switching networked systems subject to input saturation and external disturbances. *IEEE transactions on cybernetics*, 2018.
- [29] Xiangyu Wang, Shihua Li, and Peng Shi. Distributed finite-time containment control for double-integrator multiagent systems. *IEEE Transactions on Cybernetics*, 44(9):1518–1528, 2013.
- [30] MA Wiering. Multi-agent reinforcement learning for traffic light control. In *Machine Learning: Proceedings of the Seventeenth International Conference (ICML'2000)*, pages 1151–1158, 2000.
- [31] Jian Wu, Shenfang Yuan, Sai Ji, Genyuan Zhou, Yang Wang, and Zilong Wang. Multi-agent system design and evaluation for collaborative wireless sensor network in large structure health monitoring. *Expert Systems with Applications*, 37(3):2028–2036, 2010.
- [32] Feng Xiao, Long Wang, Jie Chen, and Yanping Gao. Finite-time formation control for multi-agent systems. *Automatica*, 45(11):2605–2611, 2009.
- [33] Quan Xiong, Peng Lin, Wei Ren, Chunhua Yang, and Weihua Gui. Containment control for discrete-time multiagent systems with communication delays and switching topologies. *IEEE transactions on cybernetics*, 2018.
- [34] Shuanghe Yu and Xiaojun Long. Finite-time consensus for second-order multi-agent systems with disturbances by integral sliding mode. *Automatica*, 54:158–165, 2015.
- [35] Yu Zhao, Zhisheng Duan, Guanghui Wen, and Yanjiao Zhang. Distributed finite-time tracking control for multi-agent systems: an observer-based approach. *Systems & Control Letters*, 62(1):22–28, 2013.
- [36] Zongyu Zuo and Lin Tie. Distributed robust finite-time nonlinear consensus protocols for multi-agent systems. *International Journal of Systems Science*, 47(6):1366–1375, 2016.